



# Design of a Vertical Cavity Optical Micro-Electromechanical Filter

Edwin Ataro<sup>1</sup>, Diana Starovoytova Madara<sup>1</sup>, Sitati Namango<sup>1</sup>, Augustine Makokha<sup>1</sup>, Hartmut Hillmer<sup>2</sup>

School of Engineering, Moi University, Eldoret, Kenya<sup>1</sup>

Institute of Nanostructure Technology and Analytics, Universität Kassel, Kassel, Germany<sup>2</sup>

**ABSTRACT:** Based on Micro-Opto-Electro-Mechanical System (MOEMS) technology, vertical cavity devices with an air-gap enable very efficient ultra-wide continuous tuning with only a single control parameter. The vertical cavity filters and Lasers consist of an air-gap cavity embedded between two highly reflective Bragg mirrors. Vertical Cavity Surface Emitting Lasers (VCSELs) have an active layer additionally integrated in the cavity. The ultra-wide continuous tuning is achieved by micro-electromechanical actuation of the mirror membranes. Our research activities concentrated on Bragg mirror material system with InP/air-gap mirror structures. The resonator quality depends on the refractive index contrast between the Bragg mirror layer materials and on the number of periods. The advantage of the semiconductor/air-gap system is the very high refractive index contrast ensuring a high reflectivity of more than 99.8% with only three layer periods. The semiconductor/air-gap structures forming the membranes of one Bragg mirror are *n-doped* while the other mirror membranes are *p-doped* forming a diode structure. Due to device miniaturization very efficient tuning is achieved by electrostatic actuation. The investigations presented focus on an InP/air-gap Fabry-Pérot-filter for  $\lambda_{\text{air}} = 1.55\mu\text{m}$  with an air-gap cavity thickness equal to a multiple of  $\frac{1}{2} \lambda_{\text{air}}$  embedded between two InP/air Bragg mirrors. The InP membranes have a thickness of  $\frac{3}{4} \lambda_{\text{InP}}$ , the air-gaps in between are  $\frac{1}{4} \lambda_{\text{air}}$  thick. The tuning behaviour is determined by the mechanical flexibility of the membranes and by the optical properties of the vertical cavity. The electrostatic deflection due to a reverse voltage is calculated with FEM simulations incorporating the effect of stress in the membranes. The results of the model calculations compared very well with measured values. This study describes the optical micro-electromechanical design of the novel low cost device structure applicable in optical filters, vertical cavity surface emitting lasers (VCSELs) and a host of other optical applications. We also present a solution to one of the most challenging problems in the design of micro-electromechanical devices consisting of thin-walled structures - that is residual stress. Residual stress alters device characteristics if not taken into consideration during design and characterisation.

**KEYWORDS:** surface micromachining, electrostatic tuning, optical micro-cavity filters, tuneable filter, tuneable VCSEL, membrane stress.

## I. INTRODUCTION

A wide continuous wavelength tuning of optical devices is very attractive for contemporary and future optical communication systems based on Dense Wavelength Division Multiplexing (DWDM). Examples of such systems are; the undersea optical fibre systems as well as terrestrial optical fibre communication networks. In addition, very promising applications are in optical measurements for spectrometry or gas sensing.

The phenomenal growth in communications in recent years has stimulated a great demand for innovative solutions in a bid to cost-effectively satisfy the ever growing need for larger bandwidth. DWDM has been chosen as an optimum solution towards satisfying this need [1], [2],[3],[4],[5],[6]. Communication lasers and optical filters are some of the key components of DWDM systems [7]. The choice of the type of devices for application in such a system depends on excellent performance and high reliability. Even more crucial, for the successful deployment of the devices in the market, is low cost. High production throughput especially through batch processing and high yield contribute greatly to reducing the cost. Reliable low cost fabrication technologies are therefore major pursuits for the researchers and investors in this field [8].

# International Journal of Innovative Research in Computer and Communication Engineering

(An ISO 3297: 2007 Certified Organization)

Vol. 3, Issue 4, April 2015

## II. RELATED WORK

With every new dawn, the volume of data that needs to be transmitted from one point to the other in most of the world grows almost exponentially [9]. This continues to exert more and more pressure on the available data transmission capacities. In optical communications DWDM has a place as a promising and applied technology that can be exploited to boost the aggregate system throughput. [10] Many innovators have come up with devices and technologies that can enable DWDM to be applied in transparent all-optical networks. In particular, devices and technologies such as wavelength routing switches, switched sources, tuneable Laser sources, tuneable filters, and wavelength converters have all been developed and demonstrated [10],[11],[12],[13],[14],[15],[16]. MOEMS technology has been applied in most of these cases to realise tuneable filters and Laser sources, amongst others. These devices have thin films/membranes that experience residual stress from the fabrication process. The stresses cause out-of-plane deformations that often cause the device to function unpredictably. A number of studies have been carried out to investigate and accurately characterise and control the effect of residual stress in different material systems. [17],[18],[19]. Some theoretical models have also been proposed to enable predictability and control of this stress. [17],[20], [21]. Often in the design and fabrication of MOEMS tuneable devices, the effect of residual stress is not factored in. This research work combines both in a bid to come up with more reliable devices with predictable functional characteristics.

## III. SIMULATION SETUP

### Physical and Opto-electro-mechanical design

The low cost optical multiple-membrane devices covered in this work consists of two highly reflective distributed Bragg reflectors (DBRs) separated by a resonant vertical air micro-cavity of thickness  $L = m\lambda_{\text{air}}/2$ , where  $m=1, 2, \dots$ . The DBRs consist of InP membranes that have a thickness of odd multiples of  $1/4\lambda_{\text{InP}}$ , the air-gaps in between are odd multiples of  $1/4\lambda_{\text{air}}$  thick. Fig. 1 is a schematic model of the device structure. The thickness values were determined from optical calculations which also showed that only three InP/air periods are sufficient to produce a DBR with a reflectivity greater than 99.9%. The results from simulations done using the Finite Element Method (FEM) are shown in Fig. 2. This arrangement forms a Fabry-Pérot filter. The DBRs consist of circularly shaped membranes suspended in the lateral  $x$ - $y$  plane, supported by 2, 3 or 4 beam-like suspensions [14],[15],[16] as shown in Fig. 1 and Fig. 4. These devices work as optical filters by allowing practically just one wavelength through. In addition they are tuneable, which means that the wavelength allowed through can be varied. This tuning is achieved by varying the size of the air micro-cavity. Two tested methods of achieving this are electrostatic and thermal actuation. In our case the electrostatic method was applied. Fig. 3 illustrates the tuning concept.

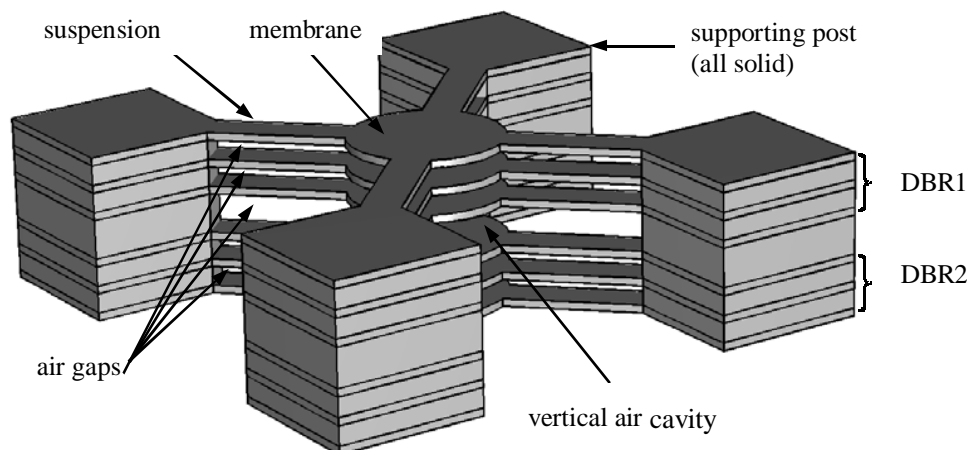


Fig.1: Structural set-up of a tuneable multi-membrane vertical air cavity optical filter structure showing circular membranes supported by 4 suspensions each. The suspensions are in turn mounted on supporting posts. The air cavity is situated between two distributed Bragg reflectors (DBRs).

# International Journal of Innovative Research in Computer and Communication Engineering

(An ISO 3297: 2007 Certified Organization)

Vol. 3, Issue 4, April 2015

In electrostatic actuation, the top and bottom DBRs are oppositely doped resulting in a *p-i-n* structure. Reverse biasing this structure results in an electrostatic attraction between the two DBRs causing a movement that changes the air cavity size. One major advantage of this method is the high continuous tuning range achieved through a single control parameter with low actuation power due to low leakage current [15],[16].

Several of these tuneable vertical-cavity multi-membrane filter devices with different structural configurations were implemented. One set had three membrane suspensions and the other four, both with membrane diameters of 20 and 40  $\mu\text{m}$ , suspension lengths between 10 and 80  $\mu\text{m}$  and suspension widths of 10  $\mu\text{m}$ . Fig. 4 shows the scanning electron micrograph of a filter structure with four suspensions.

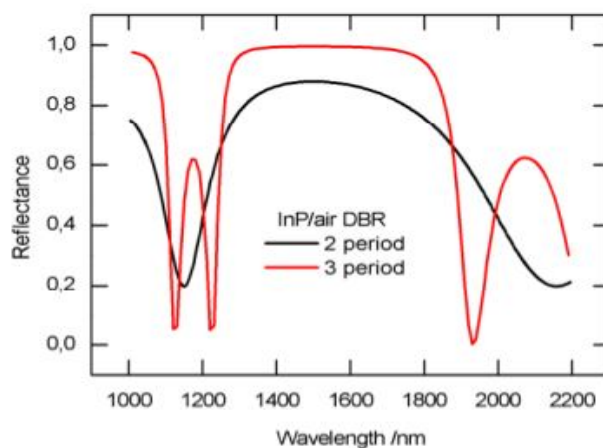


**Fig. 2:** FEM calculation results of the reflectivity of 2- and 3-period DBR mirrors. The results show a reflectivity of more than 99.9% for a DBR with only 3 periods.

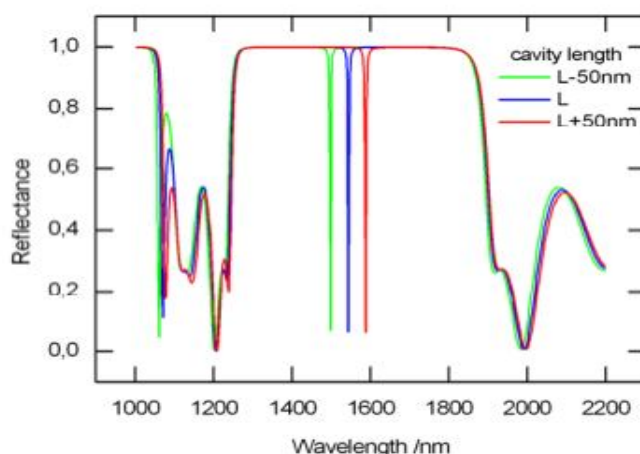


**Fig. 3:** Results of FEM calculations of the tuning characteristics of a Fabry-Pérot filter built with two DBR mirrors. Varying the air cavity length in between selects different wavelengths.

# International Journal of Innovative Research in Computer and Communication Engineering

(An ISO 3297: 2007 Certified Organization)

Vol. 3, Issue 4, April 2015

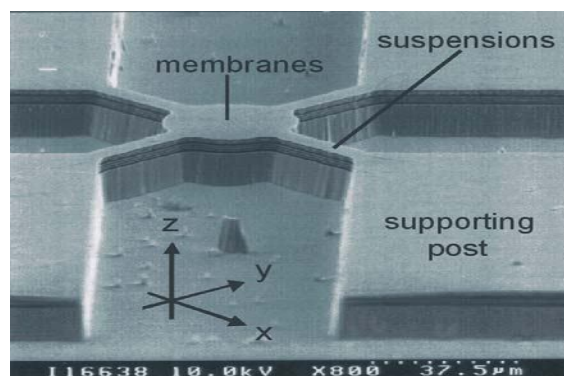


Fig. 4: The scanning electron micrograph of a filter structure with four suspensions.

## IV. RESULTS AND DISCUSSION

### 4.1. Influence of residual stress on out-of-plane deformation and tuning

Residual stress can be defined as the stress that remains in a body after the technological realisation (or after processing) that occurs in the absence of external forces or thermal influence. Residual stress can be classified into two groups [22]; Macro and micro residual stress [23], [24], [25], [26].

Two main sources of residual stress in micro-machined thin film structures are thermal stress resulting from mismatch in thermal expansion and intrinsic stress resulting from the micro-structural set-up of the film. At substrate temperatures less than a quarter of the melting point, intrinsic stress due to incomplete structural ordering dominates [27], [28], [29].

### 4.2. Control of residual stress in micromachining

Stress control in thin films is a very complex and challenging task. Some success has been reported in the control of residual stress [30]. Stress control is achieved by varying the degree of energetic particle bombardment during deposition. Compressive stress is usually attributed to atomic peening at low pressures [27], [29]. An increase in pressure increases the frequency of gas phase collisions, reducing the kinetic energy of neutral atoms impinging on the growing film. This reduction in atomic peening reduces compressive stress. The deposition pressure at which a stress reversal from compressive to tensile occur increases with the atomic mass of the element deposited [27], [29].

Residual stress has a major influence on the out-of-plane deformation of thin-walled structures, even in the absence of an external force. Residual stress can be considered to compose of mainly the axial stress and gradient stress. In the following section, results of the 3D FEM analysis of the effect of stress on a chosen structure with and without the influence of an external (in this case electrostatic) force are presented. A stress profile deduced from the deformation of a filter is extracted and used in the FEM model to calculate the tuning characteristic. This is then compared with the experimentally measured curve.

### 4.3. Effect of gradient stress and comparison with measurement

The out-of-plane deformation results mostly from gradient stress. Figure 5 shows the FEM calculated amount of out-of-plane deflection produced by various amounts of gradient residual stress without an external force, as well as the deflection when in addition an external electrostatic force is applied. The fact that the characteristics are not parallel shows that the effective stiffness of the structure is modified by the residual stress gradient.

In the following, one measurement example is analysed. This was for an all air-gap InP filter with four suspensions of  $40\mu\text{m}$  length and  $10\mu\text{m}$  width. The central membrane had a diameter of  $40\mu\text{m}$ . The membranes had a thickness  $\frac{3}{4}$  of the reference wavelength in the material. The filter was characterised by measuring the resonant wavelength for various cavity lengths. The cavity length was changed (reduced) by varying the voltage, starting from zero volts.

## International Journal of Innovative Research in Computer and Communication Engineering

(An ISO 3297: 2007 Certified Organization)

Vol. 3, Issue 4, April 2015

The design cavity was 830nm long, but with no actuation voltage applied, the measured wavelength was 1599nm. The tuning efficiency of the filter was calculated to be 0.71. The tuning efficiency is defined as the ratio of the actual wavelength change to the cavity length change during tuning. With this value, it is deduced that the actual cavity length at 0V is  $830 + (1599 - 1550)/0.71$  nm. This gives about 899nm. This increment in cavity length is caused by the residual stress. Assuming the lower and upper membranes are equally deformed in opposite direction creating a concave cavity, the amount of deflection at the centre of each membrane is about 34.5nm.

The results of Fig. 5 are used to extract the value of the gradient stress causing such a deformation. This value is then inserted in the FEM calculations to determine the tuning characteristic that takes gradient stress into account. In this work, no mechanism was in place to estimate the biaxial stress. The results therefore excluded this effect. Two characteristics were determined. The first marked “double”, assumed a symmetrical actuation of the membranes. The second one marked “single”, assumed that only one membrane moves in the actuation, the other being hindered somehow. These of course are extreme cases. The results are plotted alongside the measured values in Fig. 6. It is interesting to note that although the characteristic with symmetrical actuation shows a divergence from the measured value for large values, the experimentally measured pull-in voltage agrees almost perfectly with the calculated one. It can also be observed that the measured values lie in between the two calculated extremes. The justification of considering these extremes is that so far, no working method has been devised for determining the deformation profiles of the inner membranes in the filter, or knowing exactly what the stress profiles are. It is therefore difficult to characterise the stress in these membranes, besides no estimate of the biaxial stress was used in the calculations. The results presented here demonstrate that the treatment given is to a large extent very satisfactory.

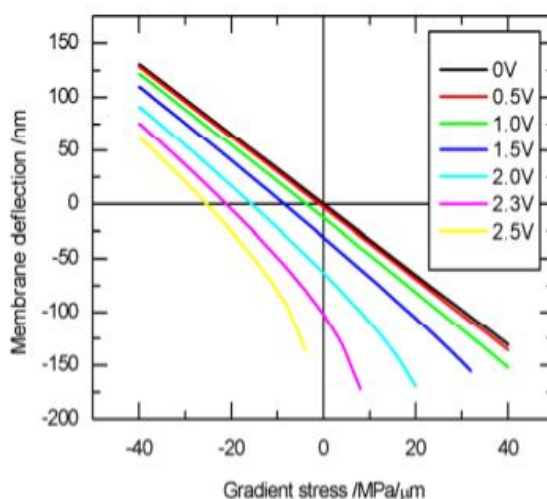


**Fig. 5:** Deflection vs gradient stress characteristics for various values of applied voltage. Negative stress gradient imply compressive stress in the top half of the membrane, tensile stress in the bottom half. The structure with four suspensions of 40 $\mu$ m length and 10 $\mu$ m width with membrane diameter of 40 $\mu$ m is considered.

# International Journal of Innovative Research in Computer and Communication Engineering

(An ISO 3297: 2007 Certified Organization)

Vol. 3, Issue 4, April 2015

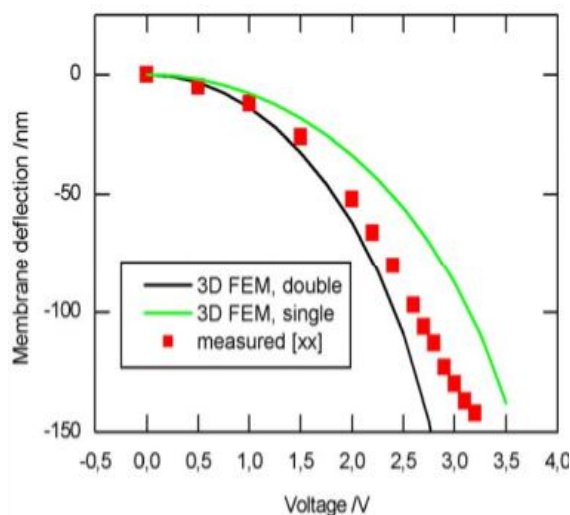


**Fig. 6:** Comparison of FEM simulated and experimentally measured characteristics for a four suspension all air-gap filter with 40 $\mu\text{m}$  and 10 $\mu\text{m}$  suspension length and width, respectively. The central membrane had a diameter of 40  $\mu\text{m}$ .

Another factor that might have affected the outcome of the calculations is the uncertainty in the value of the material parameters, in this case, the modulus of elasticity. In the literature, widely varying values for the modulus of elasticity of InP were encountered. This ranged from 61 GPa [31] to 93.41 GPa [32].

## V. CONCLUSION

In this paper a micro-electro-mechanical optical filter design is presented. It is shown that the filter exhibits excellent performance even with just three periods of the DBR mirrors used. In attempting to characterise the devices realised, it was observed that this can only be done accurately when the effect of residual stress is taken into account. An explanation of the nature and sources of residual stress has been presented. The FEM models used are modified to include the effect of residual stress. These have been used to determine the influence of stress on the out-of-plane deformation of the unactuated structures as well as on the electromechanical tuning behaviour. Comparison of model output with experimental measurements is presented showing good agreement despite neglecting the effect of biaxial stress.

## REFERENCES

1. Lucent Technologies, "Dense wavelength division multiplexing." www.iec.com, 2014.
2. C. A. Brackett, "Dense wavelength division multiplexing networks: Principles and applications," *IEEE Journal on Selected Areas in Communications*, Vol. 8, No. 6, pp. 948–64, 1990.
3. Reena Antil, Pinki, Sonal Beniwa "An Overview of DWDM Technology & Network" *International Journal of Scientific & Technology Research* Vol. 1, No.11, pp.43-46, 2012
4. A. Saleh and J. Simmons, "Technology and Architecture to Enable the Explosive Growth of the Internet", *IEEE Communications Magazine*, Vol. 49, No. 1, pp.126-132, 2011
5. E. Desurvire, "Capacity Demand and Technology Challenges for Light wave Systems in the Next Two Decades", *Journal of Lightwave Technology*, Vol. 24, No.12, pp. 4697 – 4710, 2006
6. Md. Shipon Ali, "The Challenges of Data Transmission toward Tbps Line rate in DWDM System for Long haul Transmission" *International Journal of Future Generation Communication and Networking*, Vol.7, No.1, pp. 209-216, 2014
7. J. Cavazos, "Insight into the metro's future (part 1)," Tech. rep., Frost and Sullivan, www.frost.com, August 2003
8. A. Neukermans and R. Ramaswami, "MEMS technology for optical networking applications," *IEEE Communications Magazine*, Vol. 39, pp. 62–69, 2001.
9. Mary Meeker "Internet Trends 2014" Code Conference May 28, 2014 [www.kpcb.com/internet-trends](http://www.kpcb.com/internet-trends)
10. J.M.H. Elmirghani, H.T. Mouftah, "Technologies and architectures for scalable dynamic dense WDM networks", *IEEE Communications Magazine*, Vol. 38, No. 2, pp. 58 – 66, 2000
11. Walmsley, B.A., Dell, J.M., Yinong Liu, Xiao Zhi Hu, Bush, M.B., Faraone, L., "Design and optimisation of a MEMS-based tunable Fabry-Pérot infrared filter", *Proceedings of IEEE Conference on Optoelectronic and Microelectronic Materials and Devices*, pp. 272 - 275, 01 December 2006



# International Journal of Innovative Research in Computer and Communication Engineering

(An ISO 3297: 2007 Certified Organization)

Vol. 3, Issue 4, April 2015

12. Huang, H., Liu, Y., Hu, X.Z., Bush, M.B., Winchester, K.J., Musca, C.A., Dell, J.M., Faraone, L., "Mechanical Design and Finite Element Analysis of Tunable Fabry-Perot MEMS Structures for Adaptive Infrared Detectors", Proceedings of Conference on Optoelectronic and Microelectronic Materials and Devices, pp. 205 – 208, 2004
13. Riemenschneider, F., Aziz, M., Halbritter, H., Sagnes, I., Meissner, P., "Low-cost electrothermally tunable optical microcavities based on GaAs", IEEE Photonics Technology Letters, Vol. 14, No. 11, pp. 1566 – 1568, 2002
14. E. Ataro, C. Prott, F. Römer and H. Hillmer, "Tailored Scaling: A possibility to improve the performance of ultra-wide continuously tunable photonic devices", *Applied Physics B*, Vol. 79, pp. 87-93, 2004.
15. C. Prott, F. Römer, E. O. Ataro, J. Daleiden, S. Irmer, A. Tarraf and H. Hillmer, "Modeling of Ultra-Widely Tunable Vertical Cavity Air-Gap Filters and VCSEL's", *IEEE Journal of Selected Topics in Quantum Electronics*, Vol. 9, No. 3, pp. 918-928, 2003.
16. J. Daleiden, A. Tarraf, S. Irmer, F. Römer, C. Prott, E. Ataro, M. Strassner and H. Hillmer, "Wide and continuous wavelength tuning of micro-cavity devices for optoelectronic applications", *Journal of Microlithography, Microfabrication and Microsystems*, Vol. 2, No. 4, pp. 265-274, October, 2003.
17. G. Guisbiersa, S. Strehleb, M. Wauteleta "Modeling of residual stresses in thin films deposited by electron beam evaporation", *Microelectronic Engineering*, Vol. 82, No. 3-4, pp. 665-669, 2005
18. Sanjeev K. Sharma, Deuk Young Kim, "Abnormal residual stress in nanostructured Al thin films grown on Ti/glass substrates", *Current Applied Physics*, Vol. 13, No. 9, pp. 1874-1879, 2013
19. Alireza Moridi, Haihui Ruan, L.C. Zhang, Mei Liu, "Residual stresses in thin film systems: Effects of lattice mismatch, thermal mismatch and interface dislocations", *International Journal of Solids and Structures* Vol. 50, No. 22-23, pp. 3562-3569, 2013
20. Eric Chason, "A kinetic analysis of residual stress evolution in polycrystalline thin films", *Thin Solid Films* Vol. 526, pp. 1-14, 2012
21. Yi-Ting Yu, Wei-Zheng Yuan, Da-Yong Qiao, Qing Liang, "Evaluation of residual stresses in thin films by critical buckling observation of circular microstructures and finite element method", *Thin Solid Films*, Vol. 516, No. 12, 30 pp. 4070-4075, 2008
22. I. C. Noyan, "Defining residual stress in thin film structures," *Advances in X-Ray Analysis*, Vol. , pp. 461-73, 1995.
23. F. Kandil, J. Lord, A. T. Fry, and P. V. Grant, "Review of residual stress measurement methods - a guide to technique selection," *Tech. Rep. Report MATC(A)04, NPL (National Physical Laboratory), Teddington, Middlesex, UK*, Feb 2001.
24. E. O'Brien, "Residual stress- friend or foe: A civil aircraft perspective," in *Technical Proceedings of the 2002 International Conference on Residual stress*, ICRC-6, Oxford, UK, (Oxford, UK), pp. 13-21, ICRC, 10-12 July 2000.
25. P. J. Withers and H. K. D. H. Bhadeshia, "Residual stress part 1 – measurement techniques," *Material Science and Technology*, Vol. 17, pp. 355-65, 2001.
26. P. J. Withers and H. K. D. H. Bhadeshia, "Residual stress part 2 - nature and origins," *Material Science and Technology*, Vol. 17, pp. 366-75, 2001.
27. K. O'Donnell, J. Kostetsky, and R. S. Post, "Stress control in NiV, Cr and TiW thin films used in UBM and backside metallization," in *Proceedings of IMAPS Flip-chips Conference 2002*, 2002.
28. W. Fang and J. A. Wicket, "Determining mean and gradient residual stress in thin films using micro-machined cantilevers," *Journal of Micromechanics and Microengineering*, Vol. 6, pp. 301-9, 1996.
29. J. A. Thornton and D.W. Homan, "Internal stresses in titanium, nickel, molybdenum, and tantalum films deposited by cylindrical magnetron sputtering," *Journal of Vacuum Science and Technology*, Vol. 14, pp. 164-8, 1977.
30. A. Tarraf, J. Daleiden, S. Irmer, D. Prasai, and H. Hillmer, "Stress investigation of PECVD dielectric layers for advanced optical MEMS," *Journal of Micromechanics and Microengineering*, Vol. 14, pp. 317-23, 2004.
31. S. Adachi, *Physical Properties of III-V Semiconductor Compounds*. New Jersey: John Wiley and Sons, 1992.
32. G. Jacquemod, K. Vuorinen, F. Gaffiot, A. Spisser, C. Seassal, J.-L. Leclercq, P. Rojo-Romeo, and P. Viktorovitch, "MOEMS modelling for opto-electromechanical co-simulation," *Journal of Modeling and Simulation of Microsystems*, Vol. 1, No. 1, pp. 39-48, 1999.

## ACKNOWLEDGEMENTS

Support by the DFG and BMBF in Germany is gratefully acknowledged. The authors thank C. Prott, F.Römer, J. Daleiden, S. Irmer, M. Strassner, A. Tarraf, D. Gutermuth, H. Schröter-Hohmann and I. Wensch of the Institute of Nanostructure Technology and Analytics, Universität Kassel for technical support, simulation and measurement results and stimulating discussions.

## BIOGRAPHY

Edwin Ataro is a senior lecturer at the department of Electrical and Communication Engineering, School of Engineering, Moi University. He obtained B. Tech. In Electrical & Communications 1<sup>st</sup> Class Honours in 1989, Moi University, M. Sc. Electrical & Communications, 2000, University of Kassel, Germany and Ph.D. Electrical & Informatics Faculty, University of Kassel, Germany. Research interests: photonics and optical communications, renewable energy, ICT in higher education.